

Integrating a Multibody Model and Computational Fluid Dynamics Using Mesh Motion for a Production Adapter Base Disconnection Analysis.

Marcelo Prado ¹, Gerson Brand ¹, John Hough ¹, César de Souza Lima ², and Alvaro Costa Neto ³

¹ MSC Brasil Software e Engenharia Ltda. - Rua Augusta, 1598 Cj. 41 – São Paulo – SP – Brazil

²Petrobrás S.A – CENPES – Ilha do Fundão, Quadra 7 – Rio de Janeiro – RJ - Brazil

³ Escola de Engenharia de São Carlos – USP – Av. Trabalhador São-carlense, 400 – São Carlos – SP – Brazil

Abstract: Production adapter base (PAB) is a sub sea structure used in offshore platforms to extract the oil using a high pressure natural gas injection into the well. The PAB is attached to the wellhead through the dog house lock system and, even though this is a very confident component, its fail could be very dangerous for the sea environment due to oil leakage. In order to understand the dynamics of this structure when the lock system fails a computer fluid dynamic (CFD) analysis of the gas inside the PAB's chamber and a multibody model (MBS) of the whole system were built. The gas outflow and the resultant pressure inside the PAB's chamber for each analysis condition were calculated using the CFD software. These results were imported into the MBS model and dynamic analyses were performed for critical conditions of gas pressure and deep water. The MBS model of the PAB was built taking into account all the hydrodynamic forces, added masses and drag forces.

Keywords: *Multibody, CFD, Moving Mesh, PAB*

NOMENCLATURE

ρ = fluid density, kg/m³

u = fluid velocity, m/s

ϕ = tensorial property per unit mass

q = surface source/sink

S = volume source/sink

INTRODUCTION

Experiments are an efficient means of measuring global parameters, like drag, lift, pressure drop or heat transfer coefficients. In many cases, however, it may be essential to know whether flow separation occurs, whether the wall temperature exceeds some limit or whether compressible effects have considerable influences on the system. The advantages of CFD are conditional on being able to solve the Navier-Stokes equations accurately, which is extremely difficult for most flows of engineering interest. Accurate numerical solutions for high Reynolds number flow are particularly difficult.

The objective of this work is to understand the dynamic behavior of the Production Adapter Base (PAB) when the lock system fails under different conditions of deep water and internal gas lift pressures. The application of simulation as a tool for the study of the PAB disconnection phenomenon was chosen because of the great difficulties to simulate its operational conditions in an experimental measurement.

A multibody model (MBS) using the software MSC.Adams was built to provide the mechanical simulation of the PAB disconnection and a series of steady state computational fluid dynamics (CFD) analyses using the software Star-CCM+ was run to provide the gas lift loads acting on the PAB. For the coupling of both mechanical system and fluid data, it was introduced a methodology in which the MBS model reads the gas lift data from the CFD steady state analyses. The validation of the methodology was done with a CFD analysis using the software Star-CD with moving mesh and mesh layer addition to simulate the mechanical movement of the system and the gas leakage, coupling both mechanical and fluid phenomenon.

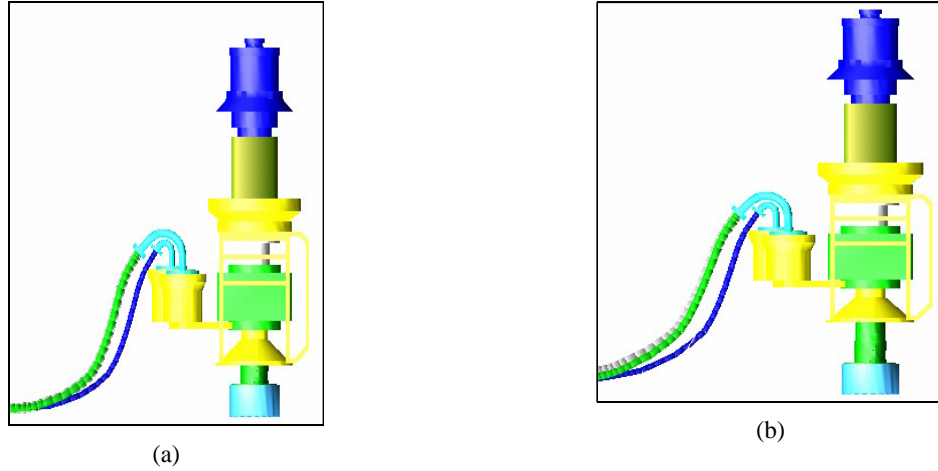


Figure 1: Disconnection analysis of the PAB on MSC.Adams environment: (a) before disconnection and (b) after disconnection.

FINITE VOLUME METHOD ON MOVING MESHES

Nowadays simulation tools can provide very useful information and a better insight into the physical processes which take place within fluid dynamics phenomenon. In some of the cases, however, there are boundaries changing during the event and this can affect the results of the fluid analysis. For these cases, there are appropriated methodologies to adapt the finite volume method (FVM) used in most common CFD software and simulate the boundary changes, including mesh motion when necessary.

In the most general cases, the mesh can be made to translate, rotate or distort in any prescribed way, by specifying time varying positions for some or all of the cell vertices. This type of mesh movement, which is sometimes referred to as “Arbitrary Lagrangian-Eulerian”, can accommodate a wide range of moving-boundary problems, such as the flow in a reciprocating-engine combustion chamber with moving pistons and valves.

For this type of problem, an additional equation called the “space conservation law” is solved for moving coordinate velocity components. This relates the change in cell volume to the coordinate frame velocity. The simultaneous satisfaction of the space conservation law and all other equations of fluid motion facilitate the general moving mesh operations performed.

The integral form of the conservation equation for a tensorial property ϕ defined per unit mass in an arbitrary moving volume V bounded by a closed surface S states (1):

$$\frac{d}{dy} \int_V \rho \phi dV + \oint_S dS \cdot \rho(u - u_b) = - \oint_S dS \cdot \rho q_\phi + \int_V S_\phi dV \quad (1)$$

As the volume V is no longer fixed in space, its motion is captured by the motion of its bounding surface S by the velocity u_b . Compared to the FVM on a static mesh, the second-order FV discretization of the Equation (1) shows only two differences: the temporal derivative introduces the rate of change of the cell volume and the mesh motion flux accounts for the grid convection. The relationship between the two is governed by the space conservation law:

$$\frac{d}{dt} \int_V dV - \oint_S ds \cdot u_b = 0 \quad (2)$$

The unstructured FMV method splits the computational space into a finite number of polyhedral cells bounded by complex polygons which do not overlap and completely cover the domain. The temporal dimension is split into a finite number of time-steps and the equations are solved in a time-marching manner. A sample cell around the computational point P located in its centroid, a face f , its area vector S_f and the neighboring computational point N are shown in Figure 2.

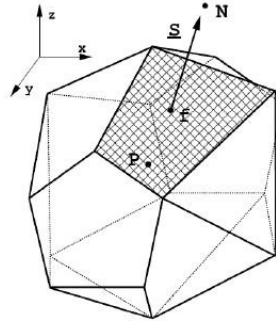


Figure 2: finite volume cell.

While Equation (2) is always satisfied in the integral form, it also needs to be preserved in the discrete form:

$$\frac{V_P^n - V_P^0}{\Delta t} - \sum_f F_s = 0 \quad (3)$$

For this reason, the mesh motion flux F_s is calculated as the volume swept by the face f in motion during the current time-step rather than from the grid velocity u_b , making it consistent with the cell volume calculation.

The mesh generated for this kind of simulation could be entirely arbitrary and there are limits on the degree of distortion that can be tolerated, imposed by accuracy and stability requirements.

In many practical applications of fluid dynamics, fluid motion is caused or regulated by the relative movement between on part of a solid body and another. This is usually accompanied by a strong inherent unsteadiness in the flow pattern. Examples of situations where such flows occur are:

- Mixing vessels;
- Turbomachinery;
- Ducted fans;
- Shi and aircraft propellers;
- Reciprocating engines;
- Trains passing through a tunnel.

The conventional numerical technique of simulating flows involving relative motion is to fix the reference frame of the solution to one of the components and solve the equations of the motion in that frame. This method can deal with only one component of motion; the rest of the components are assumed to be symmetric. Furthermore, the simulation requires experimentally-based input of some form.

By contrast, the CFD software STAR-CD permits a full transient simulation of such flows by using a sliding interface that enables cells to change their connectivity during the solution process. In the sliding interface methodology, the mesh of the solution domain is divided into two or more parts that are fixed to their respective frames of reference; say one being stationary and other moving. At the interface between these parts, the moving mesh is made to slide past the fixed one in an arbitrary fashion.

Sliding involves a continuous change in connectivity for cells on either side of the interface. This change is accommodated by indirect addressing methodology used in STAR-CD. In the treatment employed here, the two sides remain implicitly coupled during this process. Moreover, care is taken, via appropriate interpolations in time and space, to preserve flux continuity across the interface and avoid introducing spurious perturbations to the flow field.

The Arbitrary Sliding Interface (ASI) feature allows mesh mismatch across a sliding interface. This is done by allowing two or more arbitrarily-chosen adjacent portions of the mesh to slide relative to each other in small, incremental movements during the transient simulation.

There are no restrictions on the relative positions of the cell faces on either side of the sliding interface at the end of each incremental movement, i.e. vertices across the interface do not have to be coincidental. This is very useful in problems where it is difficult or impossible to ensure that one-to one correspondence between the attached boundary faces can be maintained at all times.

Some practical applications of moving meshes require a large variation in the solution domain size. In these cases, if the total number of cells in the solution domain remains fixed, the cells spacing may become too dense at some stages

or the solution and too sparse at others. This is undesirable because unnecessarily small time steps might be necessary if smaller cells are generated during the process and numerical instability problems associated with large aspect ratios of the cells.

STAR-CD overcomes these potential problems by enabling cells to be removed or added during the transient calculations. Thus, the average cell size can remain roughly constant. The general approach in removal is that mesh motion causes two or more opposing pairs of cells faces to become coincident at a specified time step, thereby causing all other faces to collapse to lines or points and thus making the cell disappear. The opposite process is used for cell addition, i.e. a previously removed cell is made to reappear.

METHODOLOGY

An initial analysis of the PAB dynamics leads us to make assumptions about the interaction between the fluid and the mechanical dynamics. The main characteristic is that the delta pressure between the gas inside the chamber and the external environment is very high. Some analyses were performed and it was verified that the fluid dynamics is much faster than the mechanical dynamics. It means that the fluid flow reaches the steady state condition after a small change in the volume domain very quickly when comparing to the vertical velocity of the PAB, allowing us to study both mechanical and fluid dynamics as uncoupled.

The assumption of studying both dynamics uncoupled lead us to run a series of steady state CFD analyses at different PAB vertical displacements and with different internal pressure of the gas inside the PAB chamber and export this data to the multibody model.

The software Star-Design was used for the mesh generation. The geometry had been prepared to be a slice part of the three-dimensional volume of control, as shown in Figure 3(a). The mesh element type chosen was the polyhedral because of its properties of faster solution using less memory and great accuracy. Figure 3(b) shows the boundary regions used in the model. Figures 4(a) and 4(b) show plots of the fluid flow in these analyses.

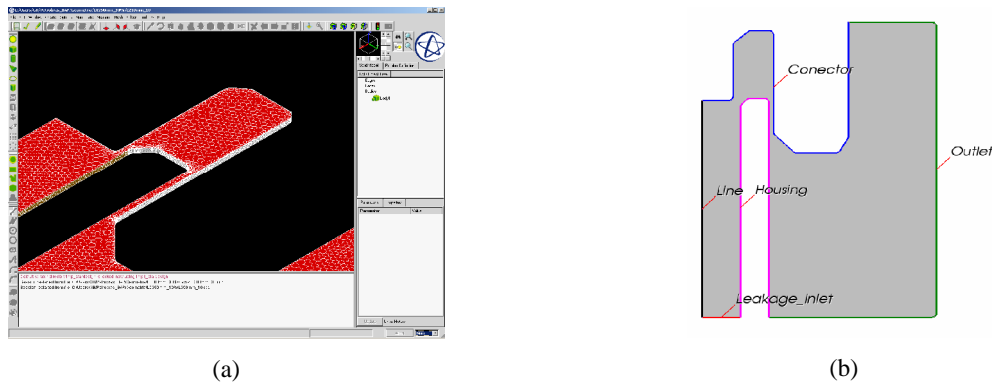


Figure 3: (a) mesh generation at Star-Design and (b) boundary regions used in the model.

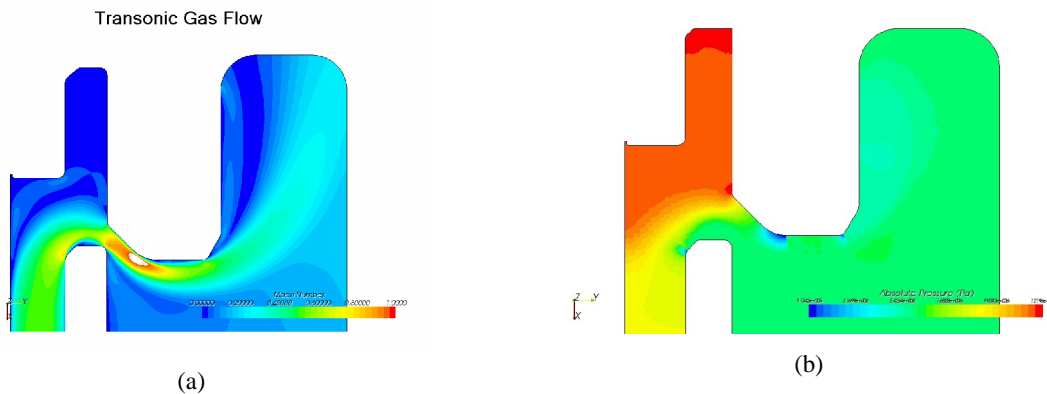


Figure 4: (a) mach number plot and (b) absolute pressure plot.

The force acting on the PAB and the mass outflow from the chamber were monitored for each configuration. Over 200 configurations were analyzed and the results were plotted on three-dimensional graphs, as shown in Figures 5(a)

and 5(b). These surfaces represent the response of the monitored parameters to all the possible conditions to occur in the system studied.

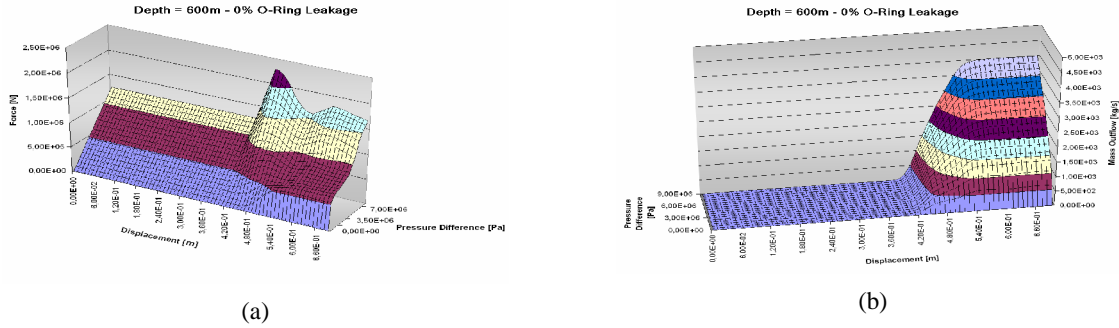


Figure 5: (a) force acting on the PAB as a function of the PAB position and pressure difference and (b) mass flow leaking from the chamber as a function of the PAB position and difference of pressure.

The results showed in Figures 5(a) and 5(b) were imported into the MSC.Adams model. At each time step, the MSC.Adams reads the information from CFD data according to the state of the system, which means instant internal pressure and PAB position, and calculates the resulting force on the PAB (Figure 6).

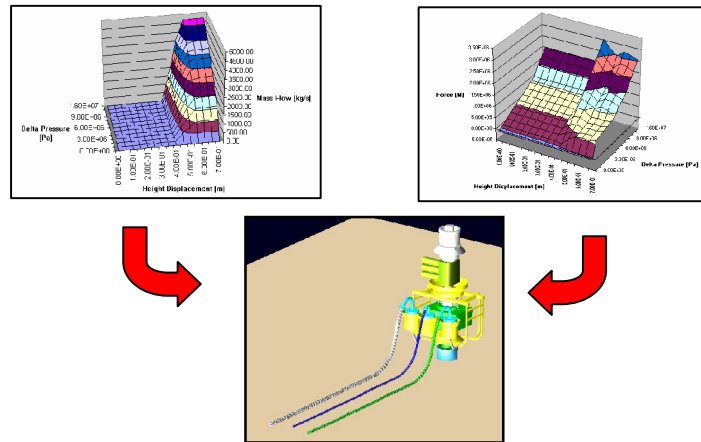


Figure 6: Integration of CFD data into the MSC.Adams model of the PAB.

The following forces were included in the MSC.Adams PAB model:

- Hydrodynamic forces:
 - Added masses forces (inertial forces);
 - Drag forces, based on Morrison’s equation;
 - Confined masses (sea water).
- Restoring forces:
 - Buyout force;
 - Wight force due gravity.
- Gas lift force based on CFD data;
- Well force due to well pressure;
- Pipeline forces due to pipelines weight and friction forces;
- Hydrostatic force due to the sea water column;
- Friction force due to oil production column.

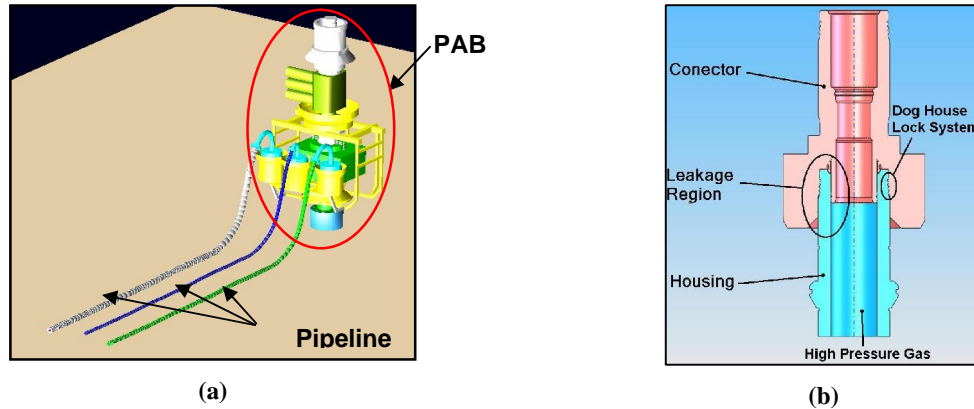


Figure 7: (a) MSC.Adams PAB model (b) description of the lock system, leakage region, well housing and PAB connector.

Discretized models of the pipelines were built using a lumped parameter approach (Figure 8). Each part of the pipeline is connected to the other part by means of beam elements. Contact forces between the seafloor and each part of the pipeline were included into the model.

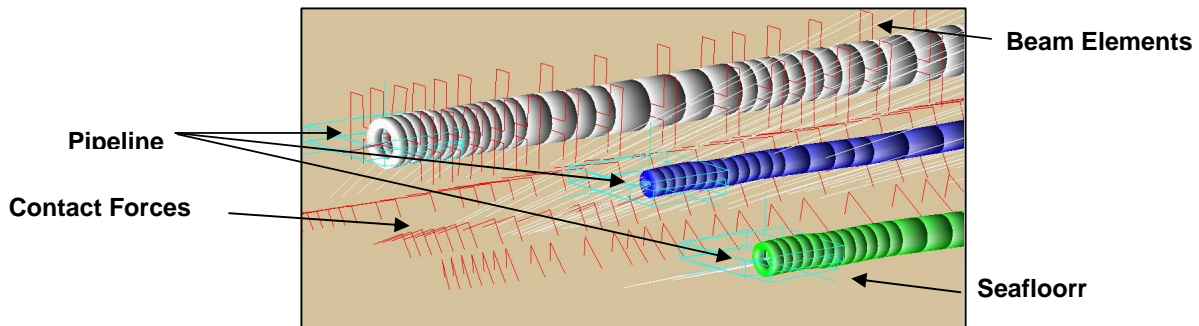


Figure 8: Lumped parameter model of the pipelines in the MSC.Adams PAB model, including the contact forces.

The validation of the methodology considering both mechanical and fluid dynamics as uncoupled was done running a transient CFD analysis using moving mesh to simulate the relative movement between the PAB and the housing, coupling in the same simulation both phenomenon.

A structured mesh was built in the software STAR-CD and it was separated in there parts, in which two of them are fixed and one is movable, as it is shown in Figure 9(a) and 9(b). It was created a sliding interface between them, which enables cells to change their connectivity during the solution process and the mesh movement.

The velocity of disconnection chosen was 1m/s, which was the worst case verified in the dynamic analyses. It was considered the lowest pressure difference between inside and outside the chamber, because this is the most favorable condition to the coupling between both phenomenons.

The results comparing steady state and transient moving mesh analyses are shown in Figure 10(a) and 10(b). It was obtained a good agreement between both approaches and the highest difference was 7.87% on the leakage gas mass flow. This result was considered sufficient to validate the methodology for this application.

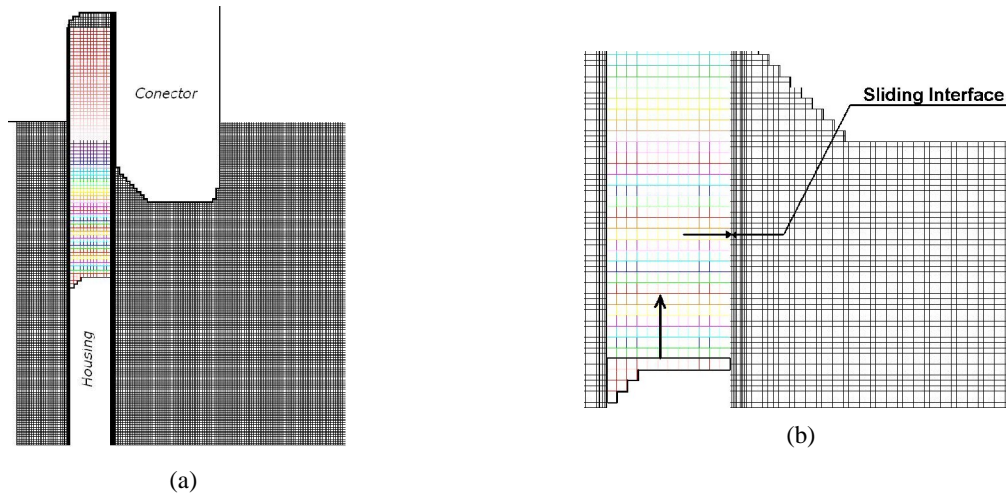


Figure 9: (a) CFD model at Star-CD and (b) representation of the sliding interface.

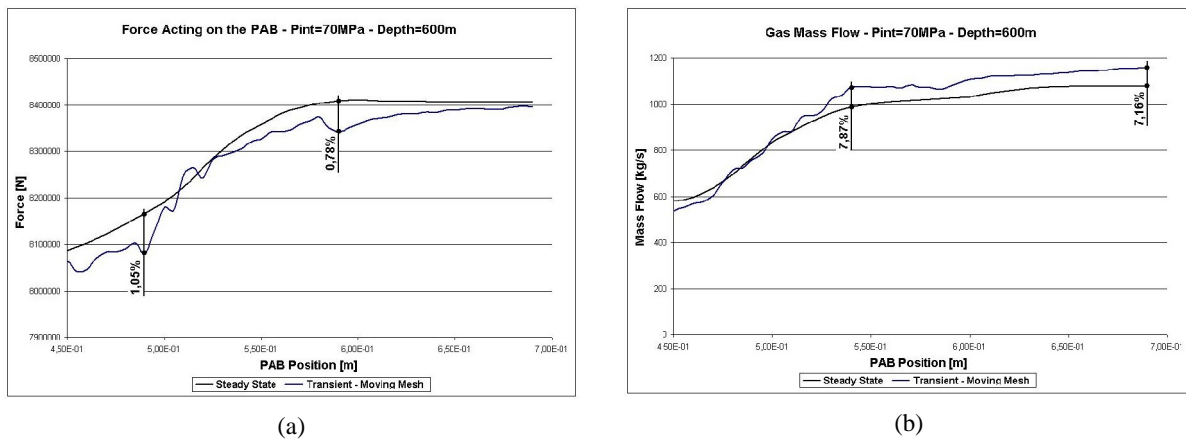


Figure 10: comparison between steady state and transient moving mesh approach of the (a) force acting on the PAB and (b) the gas mass flow leaking from inside the chamber.

RESULTS

The dynamic analyses were carried out in cases where the resulting static force on the PAB is upward. The worst case is when the gas lift pressure is 210 kgf/cm², well pressure is 60 kgf/cm² and the water depth is 800 m. The PAB areas and weighs can be seen in Table 1. Table 2 shows the added and confined sea water masses, buyout force and drag force of the production column.

Weigh PAB (kN)	Weigh Column (kN)	Gas Lift Area (m ²)	Line Production Area (m ²)	Hydrostatic Force Area (m ²)
499	505	0.128	0.0102	0.1396

Table 1: Areas and weighs of the PAB

Added Mass (kg x 10 ³)	Confined Mass (kg x 10 ³)	Buyout Force (kN)	Column Drag Force (kN)
14.4	55.3	130.5	70

Table 2: Added and confined sea water masses, buyout force and drag force of the PAB production column.

Figures 11(a) and 11(b) show the vertical velocity and vertical acceleration of the PAB. The overshoot of the acceleration in Figure 11(b) is caused by the application of the pressure due to the gas lift inside the PAB chamber on the contact area between the PAB connector and the well hub. When the vertical displacement of the PAB reaches 400 mm, the gas lift act on this area and increases the vertical force and, consequently, the vertical acceleration of the PAB.

Integrating a Multibody Model and Computational Fluid Dynamics Using Mesh Motion for a Production Adapter Base Disconnection Analysis

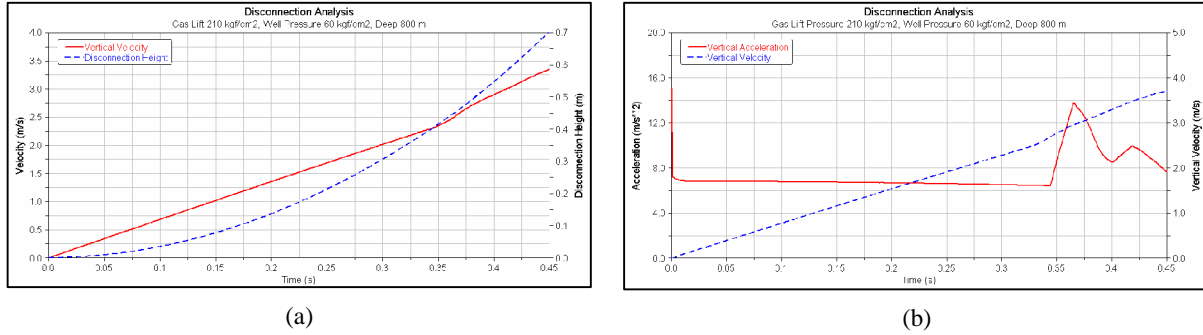


Figure 11: (a) Vertical velocity and disconnection height (b) vertical acceleration and vertical velocity.

In Figures 12(a) and 12(b) we can see that the gas lift pressure and mass outflow is constant during some time, until the PAB reaches the region (above 400 mm) when the gas lift start to flow to the outside environment.

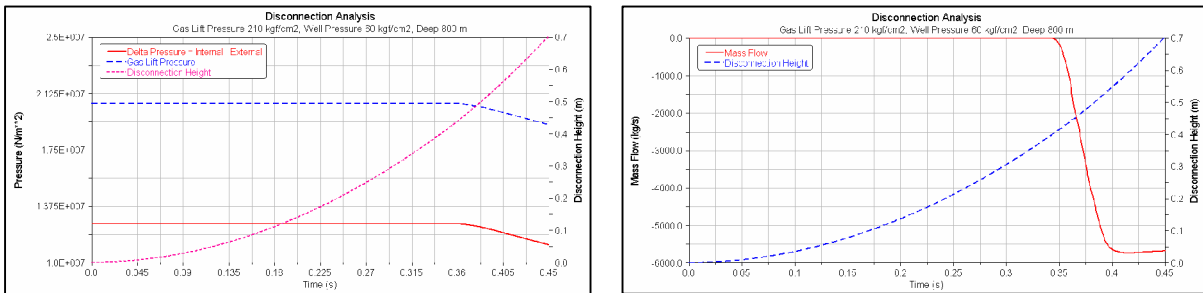


Figure 12: (a) Delta pressure, gas lift pressure and disconnection height (b) gas mass outflow and disconnection height.

Figure 13(a) shows each force acting on the PAB. As can be seen in this figure, the added and confined masses have a strong influence in the dynamic of the PAB. These inertial forces act only in the dynamic case because they are a function of the PAB acceleration. In a static analysis these inertial forces are zero. Therefore, these two inertial forces are very important to take into account in a dynamic analysis of the PAB disconnection. Figure 13(b) shows the resulting vertical forces due to pipelines attached to the PAB. These forces are very small compared to the other forces and can be neglect in a dynamics analysis.

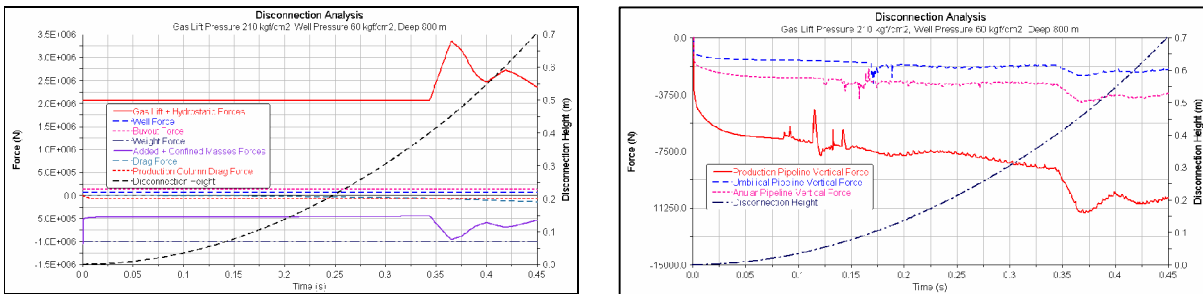


Figure 13: (a) Forces on the PAB (b) resulting vertical forces due to pipelines attached to the PAB.

CONCLUSIONS

This paper presented an approach for solving a fluid-structure interaction with great displacement to analyze the possibility of disconnection of oil Production Adapter Base (PAB) when the dog house lock system fails. The methodology used considered both fluid and mechanical dynamics uncoupled and an integration of a series of steady state CFD data and a multibody model. A transient CFD analysis with moving mesh and mesh layer addition demonstrated that it is possible to use steady-state results because the fluid dynamics is much faster than mechanical dynamics of the PAB. A very complex model of the PAB and the pipelines was built in order to evaluate the dynamic behavior of the PAB after disconnection.

REFERENCES

- Anderson, J. D., “Computational Fluid Dynamics – The Basis with Applications”, McGraw-Hill Inc., USA, 1995.
- Ferziger, J. H. and Peric, M., “Computational Methods for Fluid Dynamics”, Springer-Verlag Berlin Heidelberg, 2002.
- Lomax, H., Pulliam, T. H. and Zingg, D. W., “Fundamentals of Computational Fluid Dynamics”, NASA Ames Research Center, USA, 1999.
- Pulliam, T. H., “Solution Methods In Computational Fluid Dynamics”, NASA Ames Research Center, USA, 1986.
- Ruiz, S., Català, A., Punset, A., Arbiol, J. and Marí, R., “Multi Body System – Computational Fluid Dynamics (CFD) Integration”, 1st MSC.ADAMS European User’s Conference, London, 2002.
- Lucchini, T., D’Errico, G., “Automatic Mesh Motion, Topological Changes and Innovative Mesh Setup for I.C.E. CFD Simulations”, Dipartimento di Energetica – Politecnico di Milano, Italy, 2006.
- Star-CD Version 3.24 User Guide, CD-Adapco Group, 2004.
- Star-CD Version 3.24 Methodology, CD-Adapco Group, 2004.

RESPONSIBILITY NOTICE

The author(s) is (are) the only responsible for the printed material included in this paper.